Journal of Multidisciplinary Engineering Science and Technology (JMEST)
ISSN: 2458-9403
Vol. 7 Issue 7, July - 2020

Numerical Modeling of Cryogenic Fluid Flows in a Rocket Combustor

A Research Summary

Ryan Piersa
Department of Aerospace, Physics, and Space Sciences
Florida Institute of Technology
Melbourne, Florida

Dr. Gerald Micklow
Department of Mechanical and Civil Engineering
Florida Institute of Technology
Melbourne, Florida
gmicklow@fit.edu

***Abstract*—In this research summary, numerical models and experimental approaches for analyzing the behavior of cryogenic, turbulent fluid flows in a rocket combustor are examined and compared. One new experimental method for determining probability density functions (PDFs) for droplet size and temperature reveals that these distributions can be multimodal which challenges traditional assumptions. Numerical methods for modeling the injection process, vaporization, chemical kinetics, turbulence, combustion instabilities, and real gas effects are examined in detail. The results of the survey indicate that real gas effects become important during operation at supercritical conditions, the onset of combustion instabilities can be predicted, and the tradeoff between properly capturing the physics of the problem and saving on computational cost is the chief concern in any numerical simulation.**

Keywords—Cryogenic; Reacting; Turbulent; LES; RANS; DNS; Injection; Rocket;

I. INTRODUCTION

The recent explosion of the space industry has called for innovation and greater understanding of the complex mechanisms that occur during combustion in a rocket combustor. Due to the fact that the vast majority of rocket propulsion systems today utilize liquid propellants, modeling of the injection and combustion processes is critical to both design and operation. The replacement of costly ground tests with numerical simulations is the goal of many space agencies around the world today. The reliability, accuracy, and efficiency of these numerical simulations must improve significantly to sufficiently supplement ground testing. Many factors must be considered in the modeling of these complex processes. Some of the most important features that a good numerical model must have are an accurate representation of the injection and atomization process, a robust model of the combustion chemistry, and a precise way to determine fluid properties under both subcritical and supercritical conditions. The merging of these models into one program is a challenging ordeal and is the subject of many research programs today. One must always consider the trade-off between accuracy of the model and computational efficiency in the development of these programs.

II. MODELING OF THE INJECTION PROCESS

A. Temperature and Size Distributions of Cryogenic Droplets [3]

One of the aspects to consider when creating a numerical model for reacting cryogenic flows in a rocket combustor is how to represent the injection process. When one desires an accurate description of the atomization process of the reactants, an Eulerian-LaGrangian approach is commonly used. The liquid fuel or oxidizer droplets are tracked either individually or in computational parcels while the surrounding gas phase is modeled as a continuum. A challenging aspect of modeling the dispersed phase is how to predict the size, shape, temperature, etc. of the various liquid droplets. One approach for the prediction of these characteristics and properties is the application of probability density functions (PDFs). To determine the type of PDF to use, experimental data is required. Luo et al. conducted an experimental study where the size and temperature of liquified nitrogen, oxygen, and methane droplets were measured through the use of global rainbow refractometry (GRR) [3]. GRR is a visualization method which uses Lorenz-Mie scattering theory and the complex angular momentum (CAM) approach to obtain both the size and refractive index of individual liquid droplets in a spray. The refractive index can be used to obtain the temperature with some additional post-processing. In this work, an experimental study was conducted for turbulent flow with Reynolds numbers on the order of 104. The study found that the droplet size and temperature distributions were bimodal or even multimodal for all types studied. This information is of paramount importance in the modeling process, because it provides a basis for choosing an appropriate PDF for size and temperature distributions.

This experimental study was motivated by the increased interest in using cryogenic propellants for the purposes of rocket propulsion due to the Green

Advanced Space Propellant initiative taken up by the European Union. Cryogenic methane and oxygen are commonly chosen as alternatives to the more harmful monomethyl-hydrazine (MMH) or nitrogen tetroxide propellants. Understanding the spray behavior of these cryogenic fuels is essential for the proper and efficient operation of the propulsion system. Over the past decade, Schilerian imagery has been used to observe the behavior of these fluids at both subcritical and supercritical pressures; however, the bank of experimental data is sparse, and the present study aims to expand it through the use of a new visualization method, GRR.

The experiment was carried out for three different fluids: methane, oxygen, and nitrogen. For each test case, the fluid was liquified before injection, a pressure sensor was used to measure the inflow condition, and a thermocouple measured a time history of the fluid spray temperature. The GRR imagery setup included a laser which illuminated the flow, a lens to perform an optical Fourier transform, and an aperture for spatial filtering. A camera was then used to determine the refractive index and temperature of the droplet. The key component of the optical system was the ability to use the refractive index to determine the temperature as illustrated by figure 1:

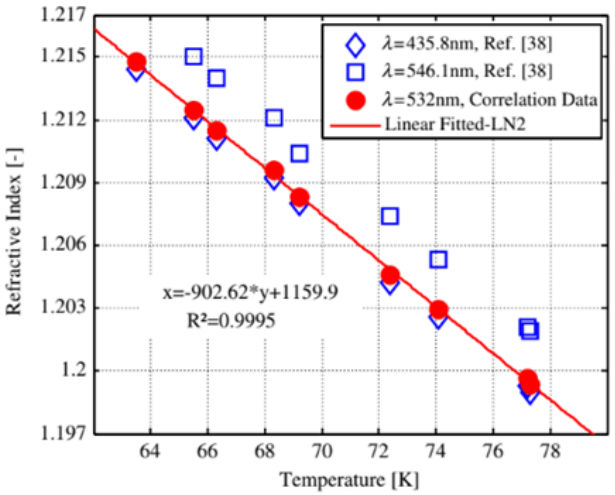

Fig 1: Refractive Index of LN2 as a function of Temperature [3]

Figure 1 shows that there is a linear relationship between refractive index of a droplet and the droplet's temperature for a specific wavelength of light. The authors of this study used this experimental data for the LN2 and LOX, and they used an experimental correlation proposed by Yoshihara et al. for the liquified methane. Two different data inversion algorithms were used in this study for the post-processing of the experimental data: the improved van Beeck method was used to obtain the mean droplet size and temperature, and Saengkaew's method was used to determine the temperature and size probability distributions.

The LN2 test was conducted at a spray Reynolds number on the order of 105 and a Weber number of 725. Based on Ohnesorge's categorization of liquid jet breakup, sprays with a Weber number larger than 40 are expected to atomize due to their own dynamic force. The droplet size distribution is shown in figure 2:

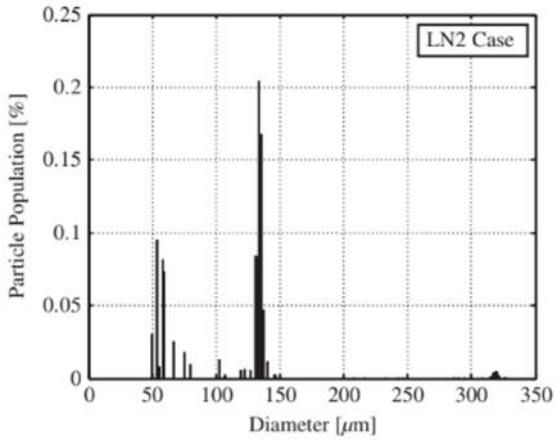

Fig 2: Droplet Size Distribution for LN2 Case [3]

The above figure shows that the probability distribution function for the droplet size is bimodal or even multimodal. The droplet sizes ranged from 50 – 320 microns with local maximums in the 50 micron and 130 micron range. This is an important result, because it indicates that a simple gaussian distribution for particle size may not be sufficient for modeling purposes. Similar results were obtained for the LOX and LCH4 cases. The LOX and LCH4 were injected at Reynolds numbers on the order of 104 and Weber numbers within the range for second wind induced atomization (13 - 40). The size distributions for the LOX and LCH4 droplets were both bimodal. The temperature measurements from the GRR method were compared to the thermocouple measurements, and the results were comparable within acceptable error bounds. A correction for heat transfer at the thermocouple tip was considered and found to be negligible.

B. Interface Tracking [8]

Another consideration for the modeling of these types of flows is how to track the non-continuous interface between the liquid and gas phase. The modeling of the liquid phase break-up through the various possible breakup mechanisms is essential in creating an accurate model for the flow in the combustor. Tani et al. simulated the combustion of gaseous hydrogen and liquified oxygen at subcritical pressures in a rocket combustor [8]. In this study, the hydrogen was injected as a gas, while the oxygen formed a liquid core. The goals of the study were to examine the atomization process, breakup of the oxygen core, and the flame holding properties of the flow. The study was conducted at subcritical pressure conditions, because many studies have already been performed at supercritical pressure conditions. The numerical method solved the 2D Navier Stokes equations in non-conservative form with the use of the Heaviside

function to track the interface location. Local equilibrium was assumed at the interface to obtain the phase change equations, and an eight species, 29 reaction model was used for the combustion chemistry. The results showed that the ignition first occurred at the rolling eddies on the leading edge of the liquid oxygen core. The shear layers ignited next, and it was observed that recirculation zones near the edge of the liquid oxygen injection post acted as flame holders. This study shows that, when operating at subcritical pressures, accurate treatment of the liquid/gas interface is essential for an accurate model of the flow.

This study considered the operation of oxygen-hydrogen rocket engines at subcritical pressures to model the start-up and shut-down processes. Many numerical studies have been conducted for supercritical combustion in these propulsion systems where turbulent mixing and diffusion dominate. For subcritical combustion, different processes, such as atomization and liquid jet breakup, dominate the flow behavior, and the investigation of these processes was the aim of the group's research. Figure 3 shows a qualitative image of the flow at subcritical conditions:

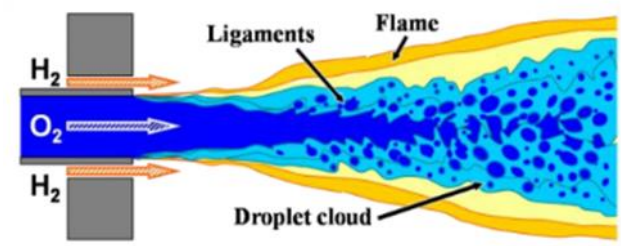

Fig 3: The Discontinuous Liquid/Gas Interface [8]

The tracking of the liquid-gas interface is of particular importance, because many numerical simulations assume instantaneous atomization of the liquid phase near the injector. While this approximation may be suitable for some injection conditions, in some circumstances, the breakup of the liquid core occurs in gradual steps and is not instantaneous.
The numerical simulation formulated in this study was conducted under the following conditions: a gas phase velocity much larger than the velocity of the liquid phase, an O/F ratio of 22.7, and a LOX injection temperature of 100 K. The influence of gas phase velocity, temperature, and density was investigated through the use of two separate trial runs. The domain is two-dimensional with grid clustering near the injector and the predicted locations of the jet shear layers. A uniform distribution boundary condition for pressure, velocity and temperature was set at the injector for both the LOX and GH2. The injector plate was assigned as an adiabatic, no-slip boundary, and the walls of the chamber were adiabatic; however, slip was allowed at the walls. The chamber outlet condition was set equal to atmospheric pressure.

The numerical model was derived from the 2D unsteady Navier Stokes equations written in the non-conservative form for homogeneous, 2 phase flow. The Heaviside function is introduced as an unknown so that a relationship between the gas phase properties and the liquid phase properties can be formulated. The governing equations for this flow, with phase change, were derived by assuming local equilibrium. To determine the amount of fluid that would change phase, both heat fluxes and mass fluxes across the interface were considered. The thermodynamic properties of the fluids at the interface were determined by selecting the relevant saturation property. The study also made use of Antoine's equation and Raoult's law for mixtures of ideal liquids for the determination of fluid properties. The chemical reaction modeling was conducted separately and explicitly in time. A detailed 8 species, 29 reaction model was used with the assumption of partial premixed flame dominance near the injector in mind.
The first major result of the numerical study was a time history of the temperature of the fluids from the time of injection to the time of ignition. One can observe the gaseous hydrogen jets developing first to be followed by the LOX core. As the LOX core breaks up, ignition sites can be seen in the rolling vortices at the edges of the core. After ignition occurs, the flames appear in the shear layers between the fluids and propagate downstream. Figure 4 shows a snapshot in time of the simulation which is taken at 1milisecond after injection:

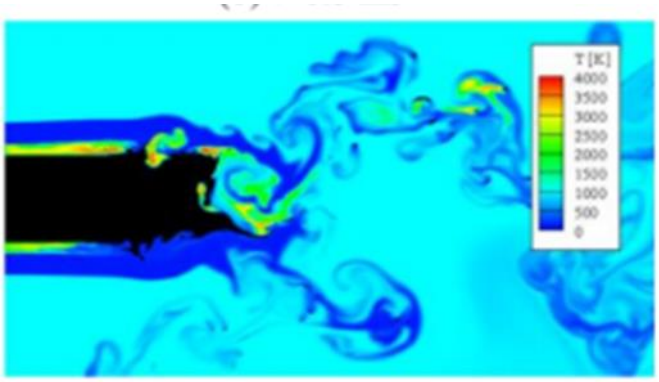

Fig 4: Snapshot of Ignition Process at t = 1 ms [8]

In figure 4, the black colored domain indicates the LOX core, while the dark blue is the gaseous hydrogen. It can be seen that the ignition takes place at the leading edge of the LOX core where the vortices that are shed roll over. These local recirculation zones can also act as flame holders for this specific instance in time.
The second major result of the study is the conclusion that the growth of instabilities in the gaseous hydrogen jets is a main driver for the breakup of the LOX core. This makes sense intuitively, because, as the hydrogen jets become turbulent, the flow obtains more kinetic energy. The turbulent jets help to break apart the LOX core through shear at the interfaces. The simulation was run to steady state, and an

interesting result is the contour of the mass fraction of hydrogen, as shown by figure 5:

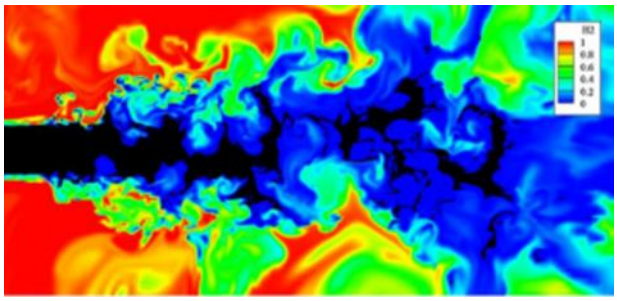

Fig 5: Mass Fraction of Hydrogen at Steady State [8]

The above figure shows that there is a large portion of unburnt fuel in the major recirculation zones of the hydrogen jets. This indicates that a rectangularly shaped combustor is not the optimal design choice, because it may lead to inefficient operation. In the design process, the combustor should be shaped such that the area of recirculation for the hydrogen jets is minimized.

C. Influence of Injector Design [9]

The study conducted by Indiana et al. considers the effect of injector design on the atomization and combustion behavior of an ethanol – hydrogen peroxide spray. Non-cryogenic propellants were studied for the purposes of simpler experimentation as well as to draw a comparison between cryogenic and storable (non-cryogenic) propellants. The two injector designs that were considered were a like doublet injector and an unlike triplet injector. The chief difference between the two designs is that the like doublet injector generates separate sprays of ethanol and hydrogen peroxide, while the unlike triplet injector creates a mixed spray. Due to the fact that impinging jet type injectors rely heavily on the jet velocity, both injector designs have the same orifice diameters, impingement distance, and impingement angle. Two experiments are conducted for each injector design: the first is non-reactive, while the second allows for combustion.

The first experiment was focused on observing the atomization behavior of the sprays. The injection pressure is regulated to control the jet velocity through an application of Bernoulli's equation. Characterization of the sprays was achieved by calculating a relevant Reynolds number, Weber number, and Ohnesorge number. Water was chosen as a substitute for the propellants in this experiment. The first result of this experiment was an experimental probability distribution function for the droplet diameter. The experiment revealed that both the droplet size PDF and Sauter mean diameter for the spray were both very similar for both injector types. This indicates that the droplet size is driven primarily by the momentum of the jet (injection pressure). Figure 6 shows the results for the like doublet injector:

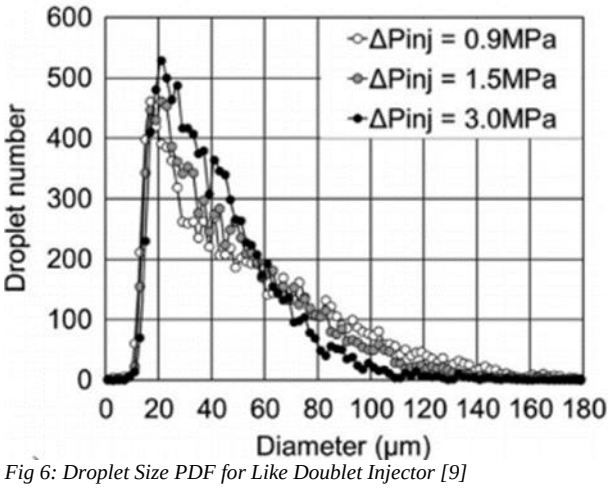

Fig 6: Droplet Size PDF for Like Doublet Injector [9]

It is worth noting that unlike the study conducted on cryogenic fuel sprays, the droplet size PDF in this study was not bimodal or multimodal. This indicates that there are significant differences in the atomization behavior of cryogenic sprays and storable propellant sprays. The results for the unlike triplet injector mirror those for the like doublet injector. This indicates that injector design does not strongly affect the mean droplet size or size distribution.

The second experiment addresses that combustion of the bipropellant mixture. The injection pressure was regulated in the same way as the atomization experiment, and the mass flow rate of each propellant is measured with a flowmeter. In this way, the equivalence ratio can be determined. The ignition source is a hydrogen-air torch which is positioned inside the injection plate. This external ignition source is required, because the bipropellant mixture is not hypergolic. Pressure and heat flux sensors are used to monitor the combustion chamber conditions during the experiment. The experimental trials were conducted at Reynolds numbers and Weber numbers that are on the order of 103. With Weber numbers in this range, full atomization of the sprays is expected. Due to the fact that the hydrogen peroxide droplets take considerably longer to vaporize than the ethanol droplets for a fixed mean diameter, the experimental strategy is to rotate the ethanol fuel spray towards the hydrogen peroxide spray so that the mixing enhances the vaporization process. This strategy is employed, because the vaporization time scale strongly drives the combustion process.

The like doublet injector relies on downstream mixing of the propellants, while the unlike triplet injector achieves propellant mixing at the impingement point. The unlike triplet injector is expected to enhance the combustion process, because the time and length scales for vaporization should be shorter than the same for the like doublet injector. The experiment revealed that this was indeed the case; moreover, the like doublet injector relied on turbulent mixing of the sprays downstream to create a vapor suitable for combustion, while the unlike triplet injector achieved

ignition in a shorter time. The major factor in the ignition delay was the vaporization of the liquid droplets. As the mean diameter of the spray increases, the vaporization time increases, and the ignition was delayed further. In terms of combustion efficiency, figure 7 shows the influence of equivalence ratio, injector design, and combustion chamber length on c* velocity and efficiency. The characteristic velocity c^* is the equal to the chamber pressure times the throat area divided by the mass flow rate.

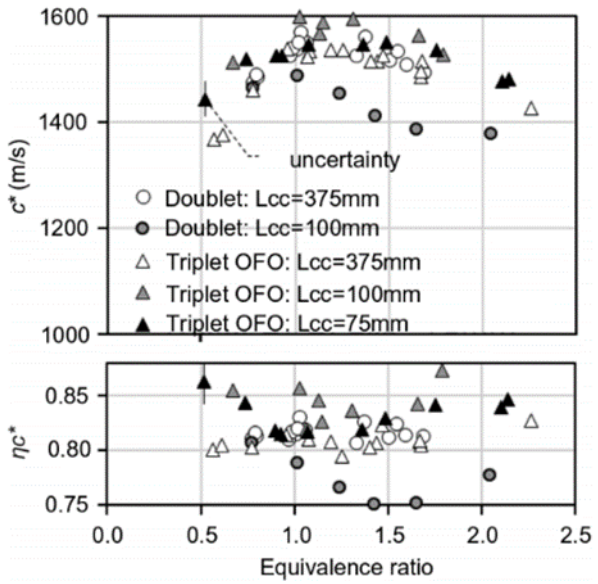

Fig 7: Combustion Efficiency [9]

The above figure indicates that the maximum c* and optimal efficiency occurs near the stoichiometric equivalence ratio. Because the difference between the peak efficiency for the like doublet injector and the same for the unlike triplet injector is less than the uncertainty in the experiment, a conclusion about which design is more efficient cannot be made. As the combustion chamber length decreases, the unlike triplet design becomes more efficient, while the like doublet design becomes less efficient. The decrease in efficiency for the doublet design is explained by a comparison of the residence time to the vaporization time. As the volume decreases, the propellants' residence time decreases. The efficiency decreases, because the propellants do not remain in the chamber for a long enough time to thoroughly mix and vaporize. The increase in efficiency for the triplet design can be explained in a similar manner, by considering that the vaporization process is not driven by turbulent mixing, and a shorter chamber has less heat loss through the walls. To completely optimize the efficiency, a study comparing residence time, vaporization time, and wall heat loss in the combustion chamber must be performed.

III. COMBUSTION MODELING

A. Comparison of Different Combustion Models [4]

De Giorgi et al. conducted a study which considered various numerical approaches for modeling the same type of fluid flow [4]. The goal of the study was to identify the best numerical approach for solving the Reynolds Averaged 2D flow field in a supercritical oxygen/methane rocket combustor. Various chemical kinetic models, solution schemes, and thermodynamic equations of state were considered with the goal of maximizing accuracy while maintaining reasonable computational time. There is little experimental data that can be used for validation of these numerical models; however, the Mascotte test bench data was used as it was the best available.

For the modeling of the chemical kinetics, the number of reactions and constituents to consider is the most important choice. Again, this choice is highly dependent on the accuracy versus computational cost trade-off. The Jones-Lindstedt (JL) and detailed skeletal (SKEL) models were compared in this study. The JL model includes 9 species and 6 reactions. In this way, the JL model is not as computationally intensive as other models. The SKEL model includes 41 reactions and is far more intensive than the JL model. It was observed that even though the JL model used far fewer reactions, the accuracy of the model was comparable to the SKEL model. The comparison between the two reaction mechanisms can be seen in figure 8:

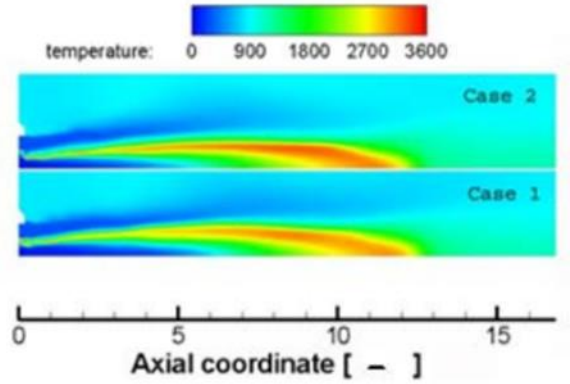

Fig 8: Temperature Contours for SKEL Model (Case 2) and JL Model (Case 1) [4]

The above figure shows that, for all else constant in the numerical models, the difference between the JL model and SKEL model is qualitatively small. This indicates that the JL model is more favorable than the SKEL model, because minimal accuracy is lost while the computational cost is drastically reduced. This is an important conclusion, because the computational cost saved here can be better spent in other areas to improve the overall accuracy of the numerical simulation. These types of comparisons are very useful in the formulation of a detailed numerical model which includes vaporization, turbulence, and chemical kinetics models.

For the chemical kinetics modeling, three approaches were considered: the eddy dissipation concept model (EDC), the chemical equilibrium PDF model, and the

PDF flamelet model. The EDC model uses the fact that in turbulent flows. The eddy kinetic energy and dissipation are crucial factors in determining the relevant chemical reaction characteristic time; moreover, turbulent mixing is a major factor in vaporizing the liquid oxidizer droplets. In this way, the reaction rates are highly dependent on the turbulent flow properties. On the other hand, the PDF models can be used in the context of chemical equilibrium or near equilibrium conditions. These approaches require careful attunement of the PDFs and a consideration of the chemical reaction times. The PDF approach is best utilized when the Damköhler number is large and the chemical characteristic times are considerably larger than the residence time. The EDC model was found to be superior to a PDF model due to the fact that in the EDC model, the reaction rates are a function of the turbulent kinetic energy and dissipation. The PDF model uses equilibrium modeling which is not as accurate as the finite rate chemistry EDC model.

The authors also considered a comparison between the Eulerian-Eulerian approach and the Eulerian-LaGrangian approach. In both cases, a real gas equation of state was required for closure when the EDC or PDF model for kinetics was used. The Peng-Robinson equation of state was used for the Eulerian-LaGrangian approach, and the Soave-Redlich-Kwong equation of state was used for the pure Eulerian approach. The results showed that the particle tracking capability of the Eulerian-LaGrangian model produced considerably more accurate results than the pure Eulerian model.

The computational domain is a rectangular, axisymmetric cross section of a circular chamber. The grid is clustered in regions of high gradients such as shear layers and wall boundaries. The simulations were performed at both subcritical and trans-critical conditions. ANSYS FLUENT was used for the simulations.

In the end, the best model for the flow was a Eulerian-LaGrangian model with the JL kinetic equations, EDC combustion, Rosin-Rammler droplet distribution function, and Peng-Robinson real gas equation of state. This study was very useful in comparing various numerical approaches to solving the same problem. The comparison to experimental data allowed for validation and confirmed the accuracy of the models.

B. Prediction of Combustion Instabilities [2]

The consideration of combustion instabilities is also essential in creating a useful and robust model for these types of flows. Having the ability to predict when these instabilities will occur can assist in the design and operation of these rocket combustors and injection manifolds. To better understand the coupling between injector design and combustion instabilities, Armbruster et al. conducted a flame dynamics study for a high-pressure oxygen/hydrogen rocket [2]. The motivation for this study comes from a discovery in industry, namely, the acoustics of the liquified oxygen injection post have been observed to cause instabilities which lead to structural failures in rocket combustors due to coupling with the frequencies of pressure oscillations and heat release in the engine. The major phenomenon investigated here is the Rayleigh criterion, which states that pressure amplitude increases when the pressure oscillations are in phase with the unsteady heat release.

The injector used in the experiment was a coaxial shear injector with a recessed, tapered post for the liquified oxygen. Two test load points were considered. The first load case was similar to that of an upper-stage engine with a thrust of 24 kN. Both test trials were conducted at Reynolds numbers on the order of 10^5.

The experimental apparatus allowed for the collection of pressure measurements at 8 different locations, and a time history of pressure readings at these locations was collected. An optical window and optical probes allowed for visualization. The optical probes take line measurements and were aligned with specific injectors or shear layers where ignition was expected. A dynamic mode decomposition was utilized to extract the dominant periodic modes from the flame radiation measurements. In this way, each mode (1st tangential, 1st longitudinal, etc.) could be investigated.

The first major result of the study was a visualization of the flow behavior in the combustion chamber. Figure 9 shows an instantaneous image of the flow:

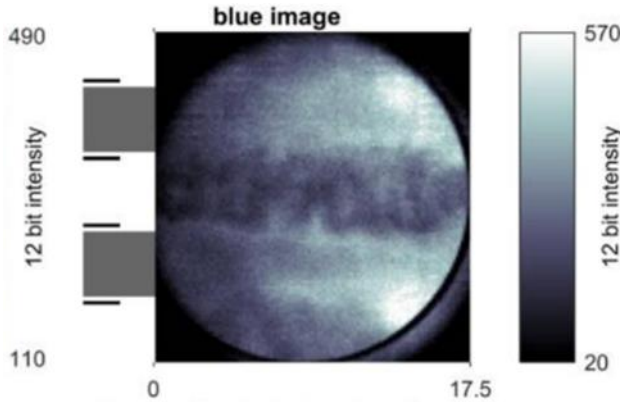

Figure 9: Instantaneous Image for Load Point 1 [2]

In the figure above, the dark section of the flow near the center of the image is the LOX core. It can be seen that the LOX core has jagged edges and is not a uniform shape. This indicates that the breakup of the liquid core occurs in segments and turbulent mixing contributes greatly to the breakup and atomization. Another important note is that downstream of the injector, the lightly colored areas indicate flame-flame interactions. This indicates that, for injectors with multiple injection ports, the flame-flame interactions

downstream may have to be modeled for certain injector configurations. The spacing between the injector ports and the angle of the sprays contribute greatly to whether flame-flame interactions should be considered or not. For the high interaction test load point, it was observed that there was a periodic variation in the liquified oxygen mass flow rate into the chamber.

The results of the study showed that once the first tangential mode of the chamber pressure oscillations approaches the frequency of the second longitudinal mode of the injector post, an effect can be observed. This was evident in the second test case (LP2), and the results are clearly summarized in figure 10:

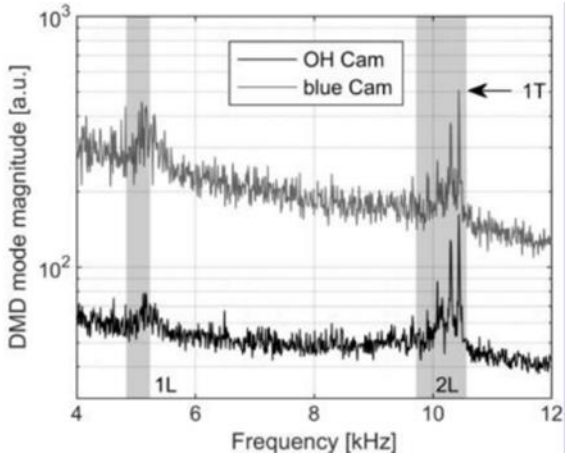

Fig 10: Flame Radiation Measurements for Load Point 2 [2]

The figure above shows the decomposition of the first tangential mode of the pressure oscillations in the combustion chamber where the longitudinal peak frequency ranges for the injection post have been indicated. One can observe that the most noticeable peak of the pressure oscillation signal occurs in the range of the peak frequency for the second longitudinal mode of the LOX injection post. This indicates that there is coupling present for this load case.

The possible source of acoustic instability of the injection post was unknown; however, the authors identified orifice whistling as the most probable cause of these instabilities. Through a calculation of the Strouhal number, the authors concluded that this whistling effect could produce a frequency that is in phase with the pressure oscillations in the chamber and thus cause issues for engine operation. The effects of cavitation in the LOX post were also investigated. A cavitation number was calculated and was large enough to justify the conclusion that cavitation is not the most probable source of these instabilities. Another possible source that was considered is noise from turbulent combustion. Due to the fact that this noise is always present, it is difficult to distinguish the effects of this phenomenon. The turbulent combustion noise is expected to contribute to the growth of instabilities, but the magnitude of this contribution relative to the hydrodynamic effects is unknown. Further study is required to identify the exact cause of these instabilities so that mitigation strategies may be developed and implemented.

IV. Numerical Simulations and Applications

A. Cryogenic Swirl Injection under Supercritical Conditions [1]

An accurate numerical model should also carefully consider how to discretize the governing equations for the appropriate flow configuration. The choice of boundary conditions and numerical solution method is highly dependent on the injector design and chamber pressure. As an example, for the consideration of these choices, Poormahmood et al. conducted a numerical study of a non-reactive cryogenic fluid flow in a 3D cylindrical chamber with a swirl-type injector at supercritical pressure [1]. The motivation for this study is that to achieve more engine power output and efficiency, operation at high pressures is required. This leads to why the behavior of these cryogenic fluids of interest must be understood at supercritical conditions.

This study focused on the formulation of a numerical model and validation through the use of experimental data. This model solved the unsteady Favre-averaged Navier Stokes equations in 3 dimensions. The density and pressure were averaged with regular time averaging, while all other flow variables were Favre averaged. The turbulence model was a hybrid model with k-ω used near the walls and k-ε used far from the walls. A turbulent viscosity model and a turbulent heat flux model were used for closure. The Soave-Redlich-Kwong equation of state was used to obtain fluid properties at supercritical conditions, and the transport properties of the fluid were obtained through the use of Chung's method. The thermodynamic properties were calculated as a sum of the ideal gas property value at the specific temperature and a correction factor which accounted for the non-ideal gas behavior.

In the simulation, liquified nitrogen was injected into a chamber pressurized by gaseous nitrogen. The inlet values for the turbulent kinetic energy and vorticity were approximated by assuming a form that is dependent on the injection velocity, turbulence intensity, and hydraulic diameter of the injector. Constant temperature boundary conditions were imposed on the chamber walls and a no-slip condition was also imposed. The domain was discretized with a staggered grid and solved with a finite volume approach. A second order upwinding scheme was used for advection terms, and an ADI scheme was employed for the treatment of the unsteady features. Figure 11 shows the results of the grid refinement study for the axial component of velocity at two different locations:

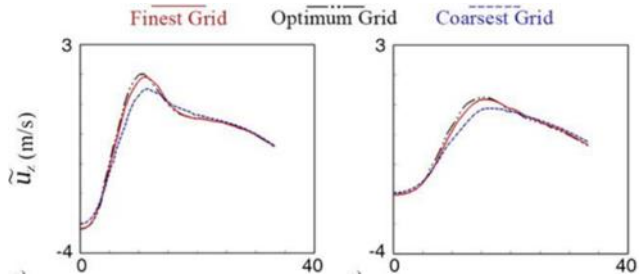

Fig 11: Grid Refinement Study for Axial Velocity [1]

The above figure shows that the time history of the axial velocity component at two different locations in space collapses to a single curve for a specific level of grid refinement. This ensures that the mesh is properly structured and will not affect the results.

The results of the study agreed well with experimental data and showed that the surrounding gas was entrained by the liquid surface and "rolled up" into the vortices. No clear interface between the gas and liquid phase could be observed due to the operation at supercritical pressure. The vortex core precesses through the domain in a helical pattern. To validate the numerical model, the spray cone angle as a function of pressure was compared to the experimental data, and a good agreement with the empirical results was observed.

The shear layer structure and behavior have a strong influence on turbulent mixing, vaporization, and ignition for cryogenic, reacting fluid flows. To investigate the structure of the shear layers, a sinusoidal wave shape was assumed for the wavy structures following the approach of Cho et al. The assumed shape of the wavy boundary as a function of distance from the injector can be seen in figure 12:

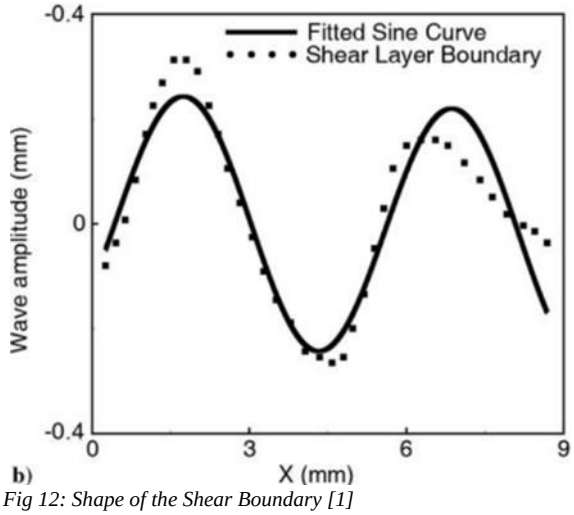

Fig 12: Shape of the Shear Boundary [1]

The discrete data points in the figure above indicate the numerical results for wave amplitude as a function of axial distance at a constant radial and azimuthal location. The fitted, sinusoidal curve for the shape of the shear boundary shows good agreement with the numerical results in general; however, the maximum amplitude and second peak amplitude is not accurately captured. These results mirror the trends of the experimental data but miss the amplitudes. This discrepancy can be attributed mostly to the turbulent viscosity model which must be adapted to accommodate the effects of cryogenic liquid injection at supercritical conditions. An interesting result is that an increase in the ambient chamber pressure results in an increase of the wave amplitude and wavelength of the shear boundary. This indicates that the chamber pressure can have a large influence on the turbulent mixing and ignition characteristics of a propellant spray under supercritical conditions.

A fast Fourier transform was used to identify Kelvin-Helmholtz instabilities as a result of pressure oscillations, and it was observed that as the chamber pressure increases, more instabilities were observed. The ability to predict these instability frequencies is important to the design and operation of the combustion chambers because of the aforementioned Rayleigh criterion.

B. Unsteady High-Order Simulation of a LOX-GH2 Combustor [5]

Lempke et al. conducted a numerical study which analyzed liquid oxygen – gaseous hydrogen combustion in a rectangular rocket combustor with a single coaxial shear injector operating at subcritical conditions. The 3D RANS equations were solved over a quarter of the combustor domain to limit computational cost. An important conclusion of the study is that the traditional axisymmetric assumption may not be the best assumption in some cases. The flame behavior, velocity field, and combustor pressure fluctuations are all addressed in this study.

The gas phase was modeled in a Eulerian framework by solving transport equations for a 3D, unsteady, compressible, turbulent, reactive flow. Favre averaging was used for the velocity, total energy, and mass fractions. The k-ω turbulence model was used, and an 8 species, 19 equation, finite rate chemistry model was chosen. An ideal gas assumption is made and is justified through comparison with the fluid properties in the NIST database. The largest discrepancy in the fluid properties from ideal gas behavior will occur in the small region that is closest to the LOX injection site. The inviscid flux variables are discretized with a flux-splitting method which also uses upwinding. The Gauss-Seidel method is used to iteratively solve the implicit equations, and a dual time stepping method is utilized to achieve time accurate results. A constant CFL number is chosen to optimize the convergence rate.

The liquid phase model is dually coupled with the gas phase. A LaGrangian, particle tracking, model is used and tracks computational parcels of droplets. Particle size, position, velocity, and temperature are computed as a function of time. All droplets are assumed to be the same shape, and vaporization is modeled as an

instantaneous mass sink. Predictor-corrector schemes are used to solve the liquid phase equations. The breakup and atomization processes are not modeled; instead, an initial droplet distribution is imposed at the injection site. These initial distribution functions are chosen in accordance with experimental results. The code was validated for kerosene injection in an air duct.

The simulation is conducted for the case of subcritical LOX injection with a prescribed turbulent velocity profile for the gaseous hydrogen at the point of injection. The adiabatic, no-slip condition is imposed at the chamber walls, and the LOX properties are obtained from the NIST database. Grid refinement is used close to the injector but could not be achieved in the shear regions.

The first major comparison made in this study is the difference between a traditional, steady state RANS simulation and an unsteady RANS (URANS) simulation. One observation is that the LOX evaporation occurs much faster in the URANS simulation at certain locations in the combustor. Figure 13 shows the amount of vaporization as a function of position in the chamber:

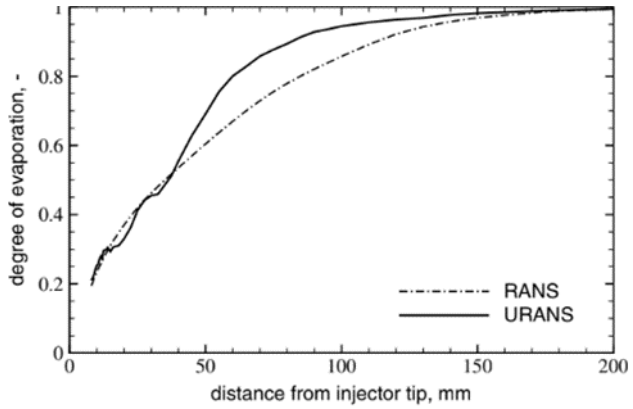

Fig 13: Evaporation Comparison [5]

The above figure shows that the RANS and URANS simulations show near identical evaporation magnitudes in the near-injector and far downstream regions. Near the center of the domain, where most of the combustion is occurring, a significant discrepancy in the amount of liquid droplets vaporizing can be observed. This discrepancy can be attributed to the enhanced combustion that occurs in the unsteady simulation.

Another interesting comparison made in this study is that between the near injector flow fields for the RANS and URANS simulations. Figure 14 shows the near injector flow field for the RANS simulation, and Figure 15 shows the same for the URANS simulation.

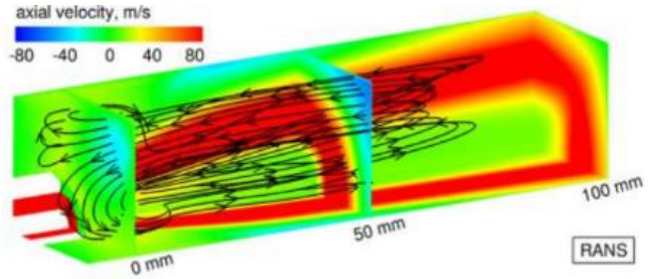

Fig 14: RANS of the Near-Injector Flow field [5]

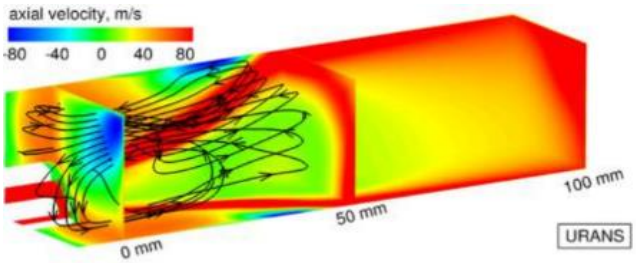

Fig 15: URANS of the Near-Injector Flow field [5]

One similarity of the two simulations is that there are considerable velocities in the circumferential direction which challenges the traditional axisymmetric assumption. The flow field is fully 3D and complex which insinuates that an axisymmetric analysis may not be sufficient in all cases. Two major vortices dominate near the injector and convect flow from the near wall region towards the core. As the flow moves downstream, counter-rotating vortices appear. The URANS simulation shows enhanced turbulent mixing which leads to faster combustion and a shorter combustor length where combustion is taking place. Also, due to the fact that the recirculation zones are smaller in the URANS simulation, less hot combustion product gas is convected to the near wall regions which leads to a buildup of cold hydrogen in the corners of the combustor. In terms of comparison to the experimental data, the flame behavior is captured far more accurately by the URANS simulation than the steady state RANS simulation. The temperature and water mole fraction profiles are also captured more accurately by the URANS simulation. The only major discrepancy is seen in the region where ignition occurs, because the URANS simulation predicts an earlier onset of combustion than what was experimentally observed. Through the application of fast Fourier transform, the pressure oscillations in the chamber were also captured accurately by the URANS simulation.

This study challenged the traditional assumption of axisymmetry by showing that the flow field can be fully 3D with substantial circumferential velocities. Also, time accurate simulations such as URANS better capture the flow behavior in the combustor. The major tradeoff is that the computational intensity is increased by a factor of 20 when performing URANS simulations rather than steady state RANS simulations. The tradeoff between accuracy and cost should always be

considered when performing these types of numerical studies.

C. *Numerical Modeling of LOX-Kerosene Combustion at High Pressures [6]*

Garg et al. conducted a numerical study of kerosene - LOX combustion in a model rocket combustor with a coaxial biswirl injector. In this configuration, the LOX is injected both axially and tangentially, while the kerosene is injected tangentially. A RANS simulation with a k-ω turbulence model, real gas equation of state, and PDF model for turbulence/chemistry interactions was performed in ANSYS Fluent. The numerical simulation was validated with experimental data from the Mascotte test facility. The study revealed that the consideration of real gas behavior is critical for systems operating at supercritical conditions.

The governing equations for the simulation were the unsteady Favre averaged Navier Stokes equations. A turbulent viscosity model was used to model the Reynolds stress term in the RANS equations. The shear stress transport (SST) k-ω method is used for the turbulence modeling. In this method, the k-ω method is used near the walls, and the k-ε model is used in the far field regions. This blending of methods has been shown to be superior to any one method for the entire domain. The combustion chemistry is assumed to be infinitely fast and driven by turbulent mixing. In this way, the entire combustion process is simulated as a mixing problem which has its own governing equation that must be solved. Chemical equilibrium is assumed at all locations in the domain, and all fluid properties become functions of the mixture fraction. A PDF is used to obtain scalar quantities such as temperature, density, etc. from the instantaneous mixture fraction.

In order to more accurately capture the real gas behavior of the flow, the Soave-Redlich-Kwong (SRK) equation of state is employed in place of the ideal gas equation of state. The agreement of the SRK equation of state with the NIST data can be seen in figure 16:

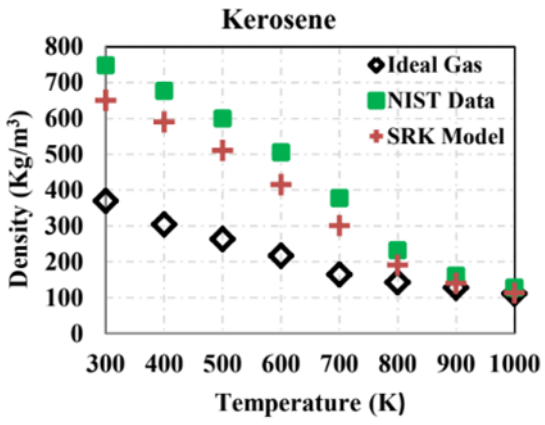

Fig 16: SRK vs Ideal Gas Equation of State [6]

The figure above indicates superior agreement of the SRK equation of state with the NIST data when compared to the ideal gas assumption. This shows that real gas behavior must be accounted for when solving these types of problems occurring at supercritical conditions.

To validate the code, results for flame shape were qualitatively compared through an observation of the OH radical distribution in the combustion chamber. For the model which used the SRK equation of state, good agreement with the experimental results was observed. A grid refinement study was also conducted to reduce uncertainty due to discretization of the domain. The first comparison made between the SRK model and the ideal gas model regarded the density variation. The SRK model more accurately captured the density distribution, and this can be attributed to the consideration of real gas behavior. The swirl velocity of the flow was another important point of comparison. Figure 17 show the swirling velocity of the flow at a chosen axial location:

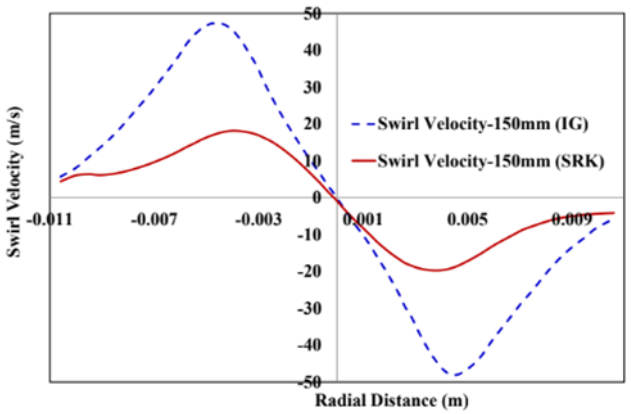

Fig 17: Swirl Velocity at 150 mm from Injector [6]

Figure 17 indicates that the magnitude of the swirl velocity was predicted to be considerably lower in the SRK model than in the ideal gas model. A larger swirl velocity would lead to a delay in the spatial mixing of the flow as a result of impeding the diffusion of the shear layers. This could inhibit combustion and provide poor agreement with experimental results. This explains the results which address the ignition and combustion zone. In the SRK model, combustion occurs quicker than in the ideal gas model due to the decreased swirl velocity magnitude.

This study indicates that the consideration of real gas behavior is essential for cryogenic reacting flows in combustors that operate at supercritical conditions. The modeling of real gas behavior through an appropriate equation of state allows for accurate prediction of velocity profiles, temperature distributions, and combustion zones which are all integral to the proper representation of the physical process. The numerical simulation conducted in this study was validated against experimental data and a

NASA code. Good predictions for the exhaust gas temperature were also made for various O/F ratios.

D. LES of Supercritical Mixing and Combustion for Rocket Applications [7]

Hickey et al. developed a numerical approach for modeling the flow behavior in a rocket combustor that is operating at supercritical conditions. This numerical model uses a large eddy simulation (LES) approach to solving the governing equations and appropriate turbulence equations. Both a non-reacting flow and a reacting flow are considered in this study. The goal is to examine the accuracy of the numerical model with regards to the proper modeling of the flow/combustion behavior in the combustor.

The first major consideration is the accurate modeling of the real gas properties. An ideal gas assumption is a poor approximation for supercritical fluids, especially in the close vicinity of the critical point. In this numerical approach, the Peng-Robinson equation of state was chosen to better capture the real fluid effects. The Peng Robinson equation of state is modified with the use of mass fractions to compute mixture properties. The thermodynamic properties are calculated as a sum of their atmospheric value and a departure function value. The departure function captures the real gas effects and is essentially a correction to the thermodynamic property based on the fluid being at a pressure other than atmospheric. Chung's method is used to calculate the dynamic viscosity of the mixture.

The numerical approach is focused on solving the spatially averaged Navier Stokes equation with a Runge-Kutta time stepping scheme. The equations are solved in their conservative form. An unstructured mesh is used, and a finite volume approach is employed. An iterative solution approach is used for non-reactive flows, and a PDF closure is used for the reacting flows.

The first simulation is for a non-reacting, trans critical nitrogen jet. The nitrogen is injected at a temperature just barely above the critical point temperature at a constant velocity. The domain is pressurized to 4 MPa. The numerical simulation agrees well with experimental data; however, the primary breakup occurs slightly further downstream in the numerical simulations than in the experiment. Numerical oscillations are prevalent in the simulation, and the inclusion of numerical viscosity would be beneficial.

The second case is for a reacting GH2/GO2 mixture. A single coaxial injector is used in this simulation, and the numerical results are compared to experimental data. The high pressure O2/H2 mechanism of Burke was used to model the combustion chemistry. The simulation was performed on both a coarse and fine grid, and the results for the streamwise velocity are shown in figure 18:

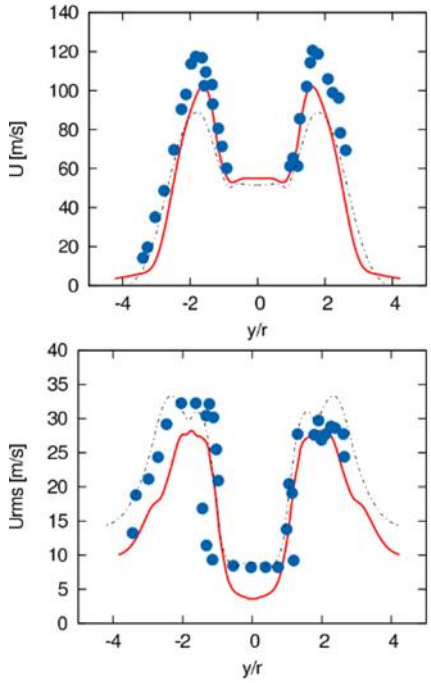

Fig 18: Streamwise Velocity and RMS for GH2/GO2 Case [7]

In the figure above, the solid red line represents the fine grid and the dashed line is indicative of the coarse mesh. The figure indicates that there is good agreement between the numerical results and the experimental data. The amplitude of the peaks for both the velocity and its RMS are not accurately captured by the numerical simulations. This discrepancy can be attributed to the numerical dissipation. Further grid refinement or the use of a less numerically dissipative method would help in reducing this discrepancy.

E. Development and Validation of Turbulent Spray Combustion Algorithm [10]

Neal et al. conducted a study with the goal of validating a numerical approach for solving the flow field in a rocket combustor. The numerical simulation employs particle tracking for the treatment of the liquid phase and an unsteady, turbulent combustion algorithm. The algorithm is based on a detached eddy simulation (DES) approach, and a flamelet model is also used. The framework used for the numerical method is a program called Loci. This programming language allows the user to specify rules and facts. With this data, the program is then able to construct a solution methodology to obtain what is desired by the user. The major advantages of this language over a traditional programming language are the ability to automatically allocate resources to parallel processors and the automatic scheduling of program events.

The particle tracking model used in this study tracks computational parcels of droplets rather than each individual droplet. In this way, computational effort can be saved by grouping similar particles together. The governing equations for the discrete phase are the

Basset-Boussinesq-Ossen equations. Three major assumptions are made in the derivation of the model: liquid phase density is much greater than the gas phase density, the particle size is small relative to the integral length scale, and shear forces are negligible with regards to particle motion. In this way, additional terms may be added to the gas phase equations to capture the effects of the discrete phase. The gas phase equations are solved in a semi-implicit manner through the use of a dissipation term for pressure which ensures the satisfaction of the continuity equation. The gas and liquid phase equations are set up to be 2-way coupled through the mass transfer term. The Langmuir-Knudsen model is chosen to represent the evaporation process, and this model is quite robust for flows with large Reynolds numbers. This model was validated by considering the time history of a water particle's diameter as it underwent vaporization. This process is shown in figure 19:

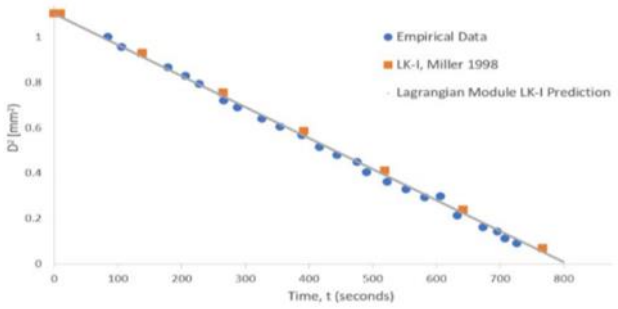

Fig 19: Time History of Change in Vaporizing Water Droplet's Diameter [10]

The figure above shows that the Langmuir-Knudsen model for vaporization exhibits excellent agreement with the experimental data. This model was also validated for an n-decane droplet and good agreement was shown in that case as well.

The validation of the code as a whole was conducted by replicating the results of an acetone jet combustion experiment. The wall boundaries were set to slip conditions, and, for the flamelet model, the mixture fraction, variance of mixture fraction, and progress variable needed to be specified at the boundaries. The variance of the mixture fraction was set to zero at all boundaries. The pilot inflow boundary values were determined by considering the stoichiometric combustion of acetone and air, and the carrier boundary values were derived from the relationship with the equivalence ratio. The mass fractions of the reactant and products were calculated before the simulation was conducted. The composition of the products was obtained through an adiabatic flame temperature calculation. These mass fractions were supplied to the code in an attempt to save the computational effort that would have been spent solving for these quantities in real time.

The major result of the study is a comparison between the empirical and numerical results of the droplet size PDF. This comparison is made in figure 20:

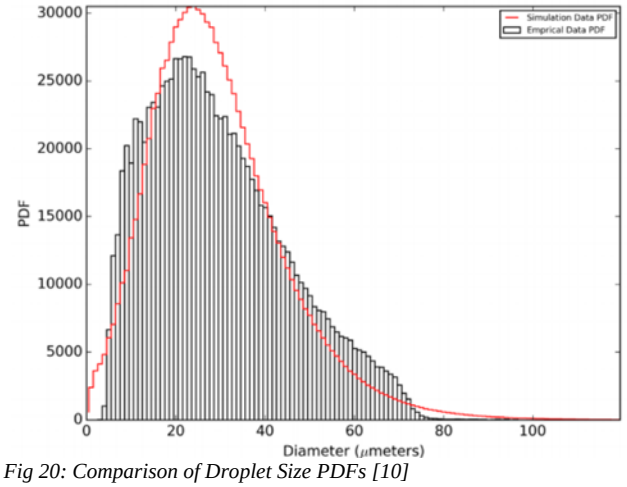

Fig 20: Comparison of Droplet Size PDFs [10]

The figure indicates that the numerical model overpredicts the number of particles with smaller diameters and underpredicts the number of droplets of larger size. The major reason for this discrepancy is that there is no coalescence model included in the numerical approach. The coalescence of smaller droplets into larger droplets must be captured to provide an accurate PDF of the droplet size. The breakup models should also be closely examined to ensure that collisions that form smaller droplets are not overpredicted. The numerical approach shows decent agreement with the experimental data. A validation of the numerical method with a cryogenic spray for comparison should be conducted to examine the robustness of the model. The assumptions made in the derivation of the discrete phase equations will be challenged in a cryogenic, supercritical environment.

V. Conclusion

This literature review addressed the challenges in experimentally measuring and numerically modeling cryogenic sprays and turbulent combustion in rocket propulsion systems. The major motivation for all of the studies examined is to replace costly and time-consuming ground tests with cheaper and faster numerical simulations. There will never be a complete substitute for a ground test; however, more advanced numerical tools can assist engineers in making the necessary design choices to optimize system performance. These studies challenged traditional assumptions such as axisymmetric flow and single-modal droplet distributions. Various methods for capturing real gas behavior, chemical kinetics, and turbulent structures were developed and validated. This field remains an incredibly active area of research today, and new numerical models are being developed across the world.

VI. Reccomendations for Future Work

The first major recommendation for future work is the implementation of bimodal or multimodal droplet size

distribution functions for cryogenic sprays. The influence of the injector design cannot be understated, and a study should be conducted which experimentally measures the droplet size PDFs for the most commonly used injector designs. A database of PDFs for size, velocity, and temperature would be incredibly valuable to numerical simulations. Another recommendation for future work would be the quantitative comparison of a numerical method which uses the axisymmetric flow assumption to a model which solves the fully 3D flow field. This comparison should be conducted for different injector configurations such as swirling, coaxial, impinging, etc. to see whether this assumption is valid under certain circumstances. A third recommendation is to study the influence of the initially specified PDF for droplet size, velocity, etc. on the behavior of the flow field in the combustor.

REFERENCES

[1] A. Poormahmood, M. Shahsavari and M. Farshichi, "Numerical Study of Cryogenic Swirl Injection Under Supercritical Conditions," Journal of Propulsion and Power, vol. 34, no. 2, 2018.

[2] W. Armbruster, J. Hardi, D. Suslov and M. Oschwald, "Injector-Driven Flame Dynamics in a High-Pressure Multi-Element Oxygen-Hydrogen Rocket Thrust Chamber," Journal of Propulsion and Power, vol. 35, no. 3, 2019.

[3] M. Luo, Y. Wu and O. Haidn, "Temperature and Size Measurements of Cryogenic Spray Droplets with Global Rainbow Refractometry," Journal of Propulsion and Power, vol. 35, no. 2, 2019.

[4] M. De Giorgi, A. Sciolti and A. Ficarella, "Application and Comparison of Different Combustion Models of High Pressure LOx/CH4 Jet Flames," Energies, pp. 477-497, 2014.

[5] M. Lempke, P. Gerlinger, M. Seidl and M. Aigner, "Unsteady High-Order Simulation of a Liquid Oxygen/Gaseous Hydrogen Rocket Combustor," Journal of Propulsion and Power, vol. 31, no. 6, 2015.

[6] P. Garg, A. Sharma, D. K. Agarwal and M. Varma, "Numerical Modeling of Liquid Oxygen and Kerosene Combustion at High Pressures," in AIAA SciTech Forum, Grapevine , 2017.

[7] J.-P. Hickey and M. Ihme, "Large Eddy Simulation of Supercritical Mixing and Combustion for Rocket Applications," in AIAA SciTech Forum, National Harbor, 2014.

[8] H. Tani, Y. Umemura and Y. Daimon, "Interface-Tracking Simulations of Liquid Oxygen/Gaseous Hydrogen Coaxial Combustion at Subcritical Pressures," in AIAA SciTech Forum, Grapevine, 2017.

[9] C. Indiana, B. Boust, M. Bellenoue and N. Azuma, "Effect of Injector Design on the Combustion of Ethanol and Hydrogen Peroxide Sprays," Journal of Propulsion and Power, vol. 35, no. 3, 2019.

[10] C. Neal, S. Thakur and J. Wright, "Development and Validation of Turbulent Spray Combustion Algorithm Using Flamelet Model in a Rule-Based Framework," in AIAA SciTech Forum, Kissimmee, 2018.